

# INVESTIGATION OF THE PRODUCTION OF COBALT-60 VIA PARTICLE ACCELERATOR

by

**Ozan ARTUN**

Department of Physics, Bulent Ecevit University, Zonguldak, Turkey

Scientific paper

<http://doi.org/10.2298/NTRP1704327A>

The production process of cobalt-60 was simulated by a particle accelerator in the energy range of 5 to 100 MeV, particle beam current of 1 mA, and irradiation time of 1 hour to perform yield, activity of reaction, and integral yield for charged particle-induced reactions. Based on nuclear reaction processes, the obtained results in the production process of cobalt-60 were also discussed in detail to determine appropriate target material, optimum energy ranges, and suitable reactions.

*Key words: particle accelerator, nuclear reaction, activity, yield*

## INTRODUCTION

The significance of the nuclear data for radionuclide production in nuclear medicine, industry, astrophysics, and cosmochemistry is considerably extensive [1-8]. Therefore, nuclear reaction and nuclear structure data are fairly important to obtain radionuclide production of top level quality. This is because the relevant production of the radionuclides is vigorously dependent on a proper knowledge of the cross-section data used to minimize the impurity level and maximize the yield of the required product [9]. The radionuclides emitting ionizing radiation are widely used for diagnosis with single photon emission computed tomography (SPECT), positron emission tomography (PET) [6, 9-12] and in therapy for intensity modulated radiation therapy (IMRT) device [13]. It is also used as gamma radiation source in different facilities such as sterilization of medical devices and radiation therapy [14]. Convenient radionuclides to identify the radionuclides which are used in more than 200 facilities, also play an important role in radiochemistry [15]. An example of nuclear data via the radiochemical techniques in the definition of yields and activation cross-sections is given for radionuclide cobalt-60 that is commercially used in the developed MRI-guided radiation therapy (MRI-GRT) to deliver IMRT [16]. Additionally, in medicine, the high dose rate (HDR) cobalt-60 brachytherapy is beneficial for the treatment of gynecological cancers, *i. e.*, cervical cancer [17]. The

calculated and measured data for the radionuclide cobalt-60, especially in the production of medical radionuclides via particle accelerator [2, 7, 18] such as diagnostic and radiation therapy, are of notable operative importance [19].

Besides the medical applications of radionuclide cobalt-60, its availability plays a significant role in radioisotope power systems (RPS) [20-22] as a potential beta source ( $\beta_{\max}$  0.318 MeV) [23, 24], occasionally called nuclear battery, for spacecraft. Therefore, the production of radioisotope cobalt-60 is important. It is produced using particle accelerator in charged induced reactions ( $p, d, t, {}^3\text{He}, \alpha$ ) on  ${}^{57,58}\text{Fe}$ ,  ${}^{59}\text{Co}$ , and  ${}^{60,61,62}\text{Ni}$  target materials.

In the present work, the production of cobalt-60 radionuclide was considered for thirteen reactions, including the cross-section, yield of product, activity, and integral yield of cobalt-60. This is because the most appropriate and inexpensive reactions for the production of cobalt-60 can be determined via activity, yield of product, integral yield, which obtain suitable incident energies of reaction and cross-section data of cobalt-60. In addition to suitable reactions, the present work focused on the fact that the calculated results proffered the best appropriate target materials for the production of cobalt-60.

## CALCULATION AND SIMULATION

To investigate the production of cobalt-60 in charged particle-induced reactions, TALYS 1.8 [25] was used for the calculations of the cross-sections of nuclear reactions. Moreover, the simulation yield of

Author's e-mails: [ozanartun@beun.edu.tr](mailto:ozanartun@beun.edu.tr)  
[ozanartun@yahoo.com](mailto:ozanartun@yahoo.com)

product and activity of reaction processes on  $^{57,58}\text{Fe}$ ,  $^{59}\text{Co}$ , and  $^{60,61,62}\text{Ni}$  target materials were carried out by particle accelerator with particle beam current of 1 mA, particle incident energy up to 100 MeV, and irradiation time of 1 h. Under these simulation circumstances, all the reaction processes were imitated by TALYS code.

In addition to the appropriate reaction for the production of cobalt-60, the suitable incident energy of these reactions was determined by integral yield using the calculated cross-section data and the mass stopping power obtained by X-PMSP program [7, 26]. Thanks to the suitable energy range of reactions, the cost effectiveness for production of cobalt-60 has decreased to minimal with suggested reactions. The investigated reactions with charged particles leading to the formation of cobalt-60 are analyzed below. However, due to deficiencies in the experimental data, those analyses lead off the experimenters in providing data.

### Material and methodology

In order to produce cobalt-60, the simulations of yield of the product and activity of cobalt-60 for all the reaction processes and irradiation on  $^{57,58}\text{Fe}$ ,  $^{59}\text{Co}$ , and  $^{60,61,62}\text{Ni}$  target materials were carried out under certain conditions. The radionuclide purity of  $^{57,58}\text{Fe}$ ,  $^{59}\text{Co}$ , and  $^{60,61,62}\text{Ni}$  target materials are 99 %, and they have uniform thickness density in all the reaction processes. However, the effective thickness values of the target materials were shifted from 0.112 cm ( $^{59}\text{Co}$ ) to 1.312 cm ( $^{62}\text{Ni}$ ), and the details are presented in tab. 1. All the reaction processes required a particle beam current of 1 mA, charged particle energy region from 5 MeV to 100 MeV, target area of 1 cm<sup>2</sup>, and irradiation time of 1 h. In addition, there was no activity loss during the reaction processes, and the maximum produced heat caused by irradiation in the target is 95 kW. After irradiation, the cooling time of  $^{57,58}\text{Fe}$ ,  $^{59}\text{Co}$ , and  $^{60,61,62}\text{Ni}$  target materials is 24 h. We simulated activity

and yield of product for the production of cobalt-60 material via nuclear reaction processes in the above conditions.

Upon taking the cross-section calculations of nuclear reaction into account, two-component exciton model of pre-equilibrium reaction (PEQ) mechanism was used. For this model, the best input parameters were used in the Fermi-gas model with constant temperature, known as CTM, for level density [25]. This mode can be defined by the following equation

$$\frac{d\sigma_k^{PE}}{dE_k} = \sigma_{CF}^{p_\pi^{max}} \frac{W_k(p_\pi, h_\pi, p_\nu, h_\nu, E_k) \tau(p_\pi, h_\pi, p_\nu, h_\nu)}{P(p_\pi, h_\pi, p_\nu, h_\nu)} \quad (1)$$

where  $E_k$ ,  $\tau$ ,  $\sigma^{CF}$ ,  $P$ , and  $W_k$  are emission energy for a particle  $k$ , the mean lifetime of the exciton state, the compound formation cross-section, the pre-equilibrium population, and emission rate, respectively. While  $p$  and  $h$  represent particle ( $p = p + p_\nu$ ) and hole ( $h = h + h_\nu$ ) numbers, and  $\nu$  are proton and neutron particles.

Regarding simulations of the activity and yield of product of nuclear reaction processes for particle accelerator, in addition to cross-section calculations, the statement for the activity of the produced isotope  $k$  can be written in terms of the nuclide inventory  $N_k(t)$  as a function of the irradiation time

$$A_i(t) = \lambda_i N_i(t) \quad (2)$$

where  $\lambda_k$  is the decay rate of ( $\lambda_k = \ln 2 / (T_k^{1/2})$ ), and  $N_k(t)$  is given by

$$N_i(t) = N_T(0) R_T \cdot i t \quad (3)$$

Thus, the activity is represented as the following

$$A_k(t) = \lambda_k N_T(0) R_T \cdot i t \quad (4)$$

where  $R_T \cdot i$  is given by

**Table 1. Obtained data of the nuclear reaction processes for the production of cobalt-60**

Target	Reaction	Target thickness [cm]	Maximum cross-section [mb]*	Energy value at maximum cross-section [MeV]	Maximum activity [MBq (mAh) <sup>-1</sup> ]	Suitable energy range [MeV]	Maximum integral yield [GBq (μAh) <sup>-1</sup> ]
Fe-57	( $\alpha, p$ )	0.126	142.25	16	3.12	–	–
Fe-58	( $t, n$ )	0.639	65.44	5	7.33	–	–
Fe-58	( $^3\text{He}, p$ )	0.160	9.19	10	0.415	–	–
Fe-58	( $\alpha, d$ )	0.129	256.09	28	14.75	–	–
Co-59	( $d, p$ )	0.760	128.34	7	27.68	–	–
Co-59	( $t, d$ )	0.557	290.83	14	110.94	–	–
Co-59	( $\alpha, ^3\text{He}$ )	0.112	59.93	44	7.99	–	–
Ni-60	( $t, ^3\text{He}$ )	0.550	163.52	42	309.69	20 60	20.58
Ni-61	( $d, ^3\text{He}$ )	0.762	69.07	51	240.79	25 70	16.05
Ni-61	( $t, \alpha$ )	0.559	448.10	46	867.65	35 70	56.94
Ni-62	( $p, ^3\text{He}$ )	1.312	44.45	45	348.47	30 80	24.17
Ni-62	( $d, \alpha$ )	0.775	92.28	70	391.99	40 85	26.03

\*1 mb = 10<sup>-31</sup> m<sup>2</sup>

$$R_{T_i} = \frac{I_{\text{beam}}}{z_p q_e} \frac{1}{V_{\text{tar}}} \int_{E_{\text{back}}}^{E_{\text{beam}}} \frac{dE}{dx} \sigma_i^{TP}(E) dE \quad (5)$$

where  $I_{\text{beam}}$ ,  $V_{\text{tar}}$ , and  $\sigma_i^{TP}$  represent beam current, active target volume, and residual production cross-section of  $k$ , respectively.  $z_p$  and  $q_e$  represent the charge projectile charge number and the electron charge.

Based on the cross-section calculation of reactions, yield calculations for the charged particle-induced reactions in the production of radionuclides between  $E_1$  and  $E_2$  energy range are calculated by the activation equation given below [9]

$$A \frac{N_L H}{M} I (1 - e^{-\lambda t}) \int_{E_1}^{E_2} \frac{\sigma(E) dE}{dE/d(\rho x)} \quad (6)$$

where  $N_L$ ,  $M$ ,  $I$ , and  $H$  are the Avogadro number, mass number of the target element, projectile current, and isotopic abundance of target nuclei, respectively,  $dE/d(\rho x)$  is the mass stopping power ( $\text{MeVcm}^2\text{g}^{-1}$ ) named as  $S_p(E)$ ,  $\lambda$  – the decay constant of the product,  $t$  – the time of irradiation, and  $\sigma(E)$  – the cross-section value at energy  $E$ .

To determine the mass stopping powers for proton, deuteron, triton, helium-3, and alpha-charged particles on target materials, we utilized X-PMSP program using the following method [7, 26].

$$\frac{dE}{\rho dx} = 0.3071 \frac{Zz^2}{A\beta^2} \ln \left( \frac{\beta^2}{1 - \beta^2} \right) + \beta^2 \ln(I) + \frac{\delta}{2} \quad (7)$$

where particle velocity  $\beta$  equals to  $\mathcal{V}/c$ .  $A$ ,  $Z$  and  $I$  are mass number, proton number, and the mean ionization potential of target, and  $\delta$  represents density effect corrections. Formulation of the mass stopping power is strongly dependent on parameters  $I$ ,  $X$ , and  $\delta$ , and their values are given in detail in a previous study [7].

## RESULTS AND DISCUSSION

### Calculation of cross-sections

The cross-section for the production of cobalt-60 for 12 nuclear reactions with charged particle-induced reactions on  $^{57,58}\text{Fe}$ ,  $^{59}\text{Co}$ , and  $^{60,61,62}\text{Ni}$  target materials are calculated in  $E_{\text{particle}}$  100 MeV range and are depicted in fig. 1. The maximum points of calculated cross-section of all reactions are lower than 50 MeV, and the results show that a particle accelerator with  $E = 50$  MeV can be taken into account to produce cobalt-60.

To analyze and understand additives of nuclear reaction process, the production of cobalt-60 requires reliable cross-section calculations. The prediction and analysis of nuclear reactions can be ensured through

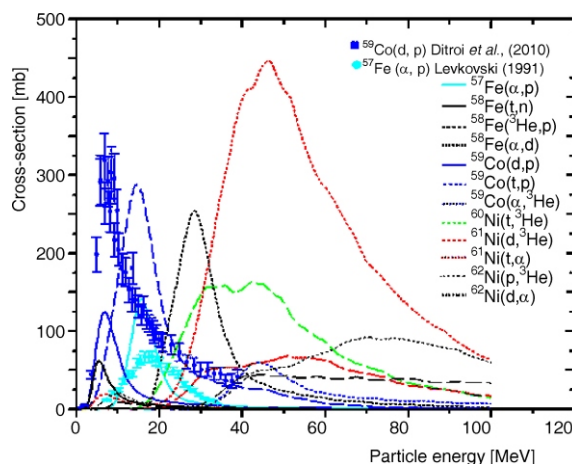


**Figure 1. Calculated cross-section for the formation of  $^{60}\text{Co}$  in the charged particle induced reactions on different targets**

trustworthy computer codes. For this aim, the calculations and simulations of nuclear reaction processes were presented using TALYS code and the calculated results were compared with the experimental data obtained from EXFOR [27]. Because, this code is one of the most important code in literature, it brings about formation of TENDL [28], which is nuclear data library providing the results of TALYS code, to be compared to the experimental measurements and other theoretical results. For example, Detroi *et al.*, [29] investigated deuteron-induced reaction on cobalt target and noted that the results of the TALYS/TENDL generally offer the best results among the available theoretical codes [29]. Regarding the production of Co-60, there are weak experimental cross-section data to compare the theoretical results. However, the calculated cross-sections for  $^{57}\text{Fe}(\alpha, p)$  and  $^{59}\text{Co}(d, p)$  reactions were compared with the measurements by Levkoski [30] and Detroi *et al.* [29], respectively. The data reported by Detroi *et al.* are higher than those of the theoretical results, however the maximum value of cross-section curve for both experimental data and theoretical result gave  $\sim 6$  MeV incident particle energy. The reported cross-section by Levkoski for  $^{57}\text{Fe}(\alpha, p)$  is lower beyond 12 MeV than the calculated results, and the energy value that corresponds to the maximum cross-section value is between 15 MeV and 18 MeV incident alpha energies. The cause of low cross-section curve could be because each sample in Levkoski's experiments was in the form of an oxide and was coated with an aluminum foil. Furthermore, regarding the difference between theoretical results and experimental data, especially, at the maximum of the cross-section values or the yields, experimentally obtained data can be different from theoretical results because of experiment radiation damage effects, not homogenous incident particle beam, unsanitary measurements, *etc.* [9].

As can be observed, the highest cross-section curve to produce radioisotope cobalt-60 in alpha, triton,  $^3\text{He}$ -induced reactions on  $^{57,58}\text{Fe}$  target is  $^{58}\text{Fe}(\alpha, d)$  at

29 MeV. Its value is about 250 mb, the  $^{58}\text{Fe}(^3\text{He}, p)$  reaction is close to zero, and the cross-section curve of the other reactions for  $^{57}\text{Fe}$  and  $^{58}\text{Fe}$  targets are 145 mb and 60 mb in 18 MeV and 6 MeV, respectively. It is worth mentioning that there are (d, p), (t, d) and ( $\alpha$ ,  $^3\text{He}$ ) reactions on  $^{59}\text{Co}$  target. The highest value (290 mb) is for (t, d) reaction at 14 MeV incident energy.  $^{61}\text{Ni}(t, \alpha)$  has the highest cross-section value (about 450 mb) in the incident energy of 45 MeV. Figure 1 shows that the cross-section curves of  $^{59}\text{Co}(t, d)$  and  $^{58}\text{Fe}(\alpha, d)$  reactions cut off each other in certain energy ranges, which are 9-22 MeV and 22-33 MeV, respectively. In the case of  $^{60}\text{Ni}(t, ^3\text{He})$ , the cross-section curve of reaction is fairly wide and not sharp. It is clear that optimal production of reactions is related not only to cross-section but also to activity and yield. Thus, the calculations of the reactions' cross-section to be produced by the suitable reaction of the radioisotope cobalt-60 are not sufficient alone. Hence, in addition to reactions cross-section, the activity (fig. 2) and yield of product (fig. 3) processes should also be investigated for all the charged particle-induced reactions.

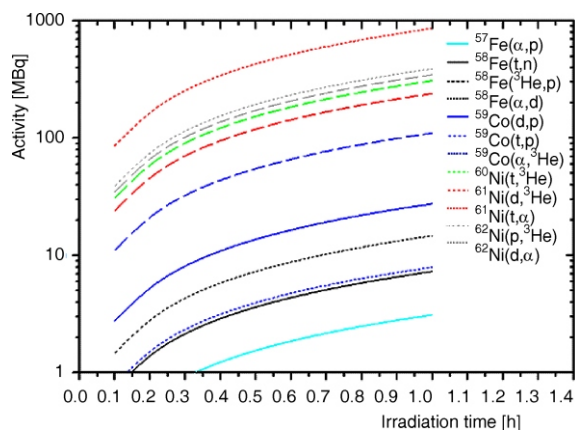


Figure 2. Simulated activity of  $^{60}\text{Co}$  as a function of irradiation time

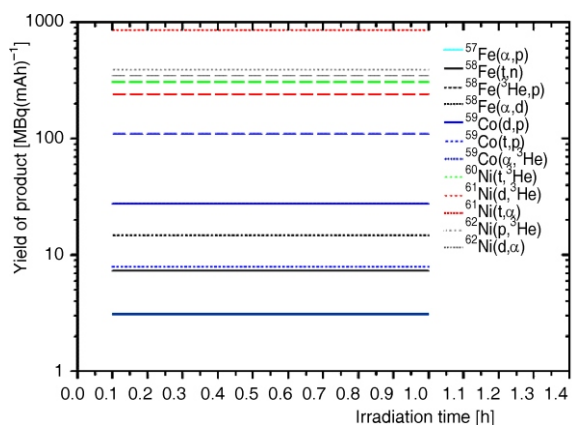


Figure 3. Simulated yields of  $^{60}\text{Co}$  as a function of irradiation time

## Simulation of activities and yields of product

For an accurate determination of the production of the radioisotope cobalt-60, the simulated results for the yield of product and activities of the charge particle-induced reactions via a particle accelerator for the dependence of the irradiation time are shown in figs. 2 and 3. In figs. 2 and 3, the cross-section curve of the  $^{61}\text{Ni}(t, \alpha)$  reaction is in agreement with the activity and yield of cobalt-60 curve because its values correspond to the highest yield and activity. However, for some reactions, this situation is not applicable for  $^{59}\text{Co}(t, d)$  ( $110.9 \text{ MBq(mAh)}^{-1}$ ) and  $^{58}\text{Fe}(\alpha, d)$  ( $14.8 \text{ MBq(mAh)}^{-1}$ ). While  $^{58}\text{Fe}(\alpha, d)$  reaction in cross-section calculation is higher than lots of reactions in term of the results of yield and activity, it has considerably low curve and another interesting point. The charge particle induced reactions for production of cobalt-60 on Ni target have the highest activity and yield of product compared to other reactions.

On the other hand, the appropriate target material for production of radioisotope cobalt-60 is  $^{60,61,62}\text{Ni}$ , which are stable isotopes of Ni. Therefore, those isotopes as target can be reliably recommended for the production of cobalt-60, and  $^{60}\text{Ni}(t, ^3\text{He})$ ,  $^{61}\text{Ni}(t, \alpha)$ ,  $^{61}\text{Ni}(d, ^3\text{He})$ ,  $^{62}\text{Ni}(p, ^3\text{He})$ , and  $^{62}\text{Ni}(d, \alpha)$  can be proposed as suitable reactions.

## Calculation of integral yield

The integral yield of radioisotope cobalt-60 in triton, proton, and deuteron-induced reactions on Ni target in the energy range from 5 MeV to 100 MeV is calculated from the cross-section and the mass stopping power obtained in figs. 1 and 4. The suitable energy range of the reactions to produce cobalt-60 can be explained by calculated integral yield presented in fig. 5, where optimum energy for  $^{61}\text{Ni}(t, \alpha)$  reaction is within the range from 35 MeV to 70 MeV, and over optimum energy amounts to  $\sim 41.6 \text{ GBq}(\mu\text{Ah})^{-1}$ . The optimum energies of  $^{61}\text{Ni}(d, ^3\text{He})$  and  $^{60}\text{Ni}(t, ^3\text{He})$  reactions are within the ranges of 25 MeV to 70 MeV and 20 MeV to 60 MeV, where the production of cobalt-60 is more than 90 %. It has been noted that the integral yield values for the optimum energy range of these reactions are  $\sim 10.5 \text{ GBq}(\mu\text{Ah})^{-1}$  and  $\sim 13.7 \text{ GBq}(\mu\text{Ah})^{-1}$ . The cobalt-60 produced by  $^{62}\text{Ni}(p, ^3\text{He})$  and  $^{62}\text{Ni}(d, \alpha)$  reactions has high energy range, and thus, the suitable energy of  $^{62}\text{Ni}(p, ^3\text{He})$  and  $^{62}\text{Ni}(d, \alpha)$  reactions appear to be more than 100 MeV due to increasing yield value. However, the integral yield values of  $^{61}\text{Ni}(d, ^3\text{He})$  and  $^{60}\text{Ni}(t, ^3\text{He})$  amount to  $\sim 16 \text{ GBq}(\mu\text{Ah})^{-1}$  and  $\sim 20.5 \text{ GBq}(\mu\text{Ah})^{-1}$  at 100 MeV.

## CONCLUSIONS

The present work has clearly researched the optimum energy range and the suitable reactions to pro-

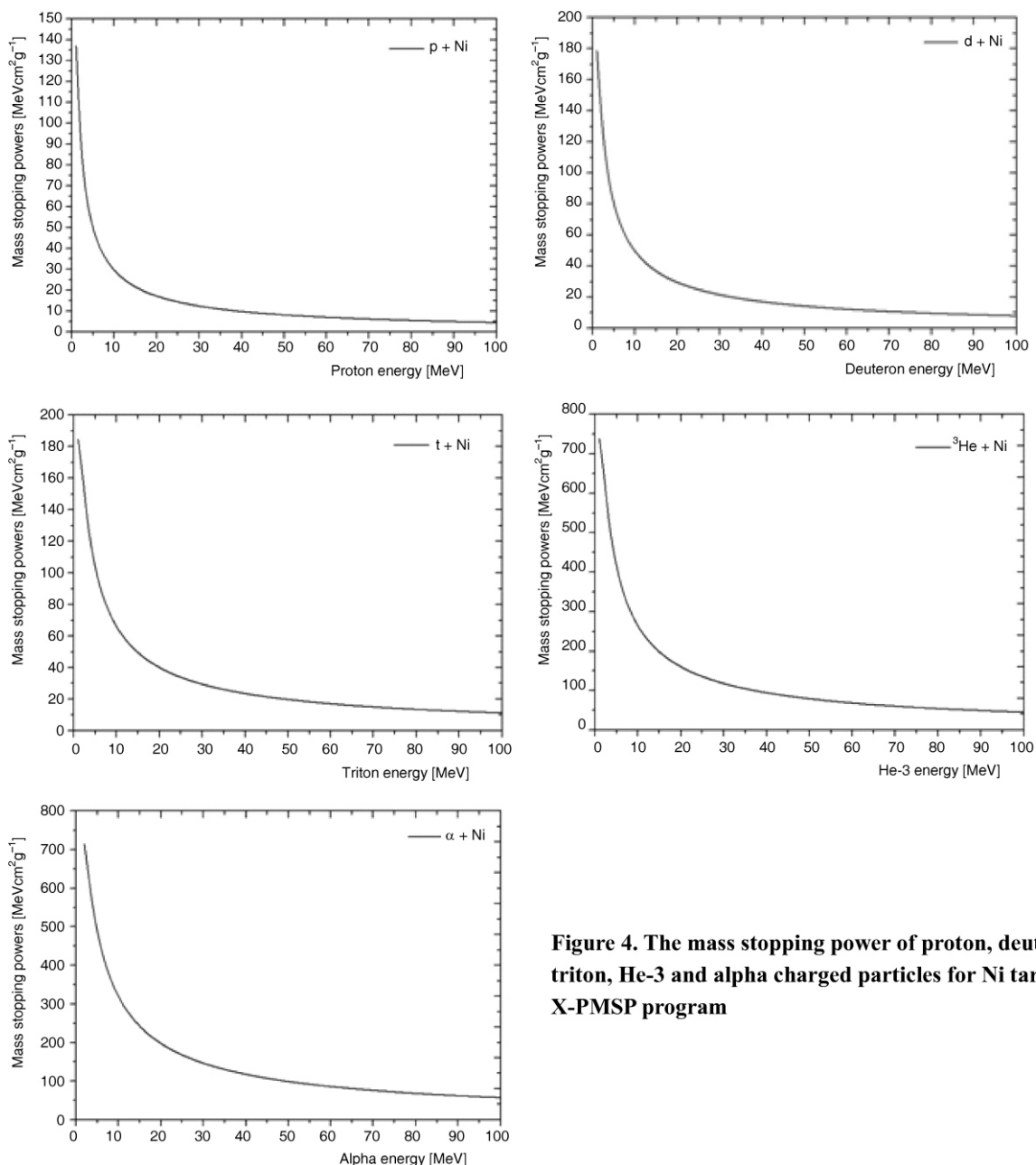


**Figure 4. The mass stopping power of proton, deuteron, triton, He-3 and alpha charged particles for Ni target via X-PMSP program**

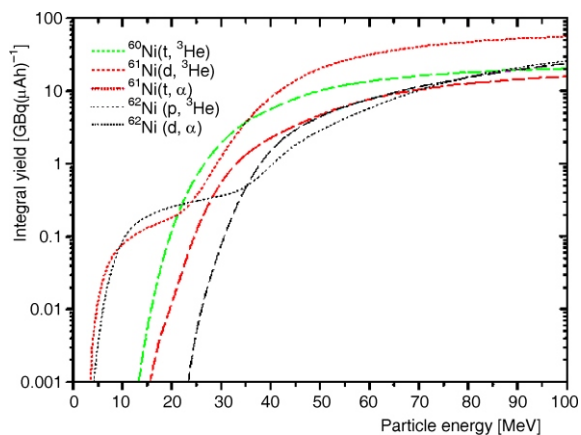


**Figure 5. Calculated integral yield of <sup>60</sup>Co as a function of energy**

duce cobalt-60 via particle accelerator for use in cancer therapy as gamma source. Cobalt-60 is also used in RTG of spacecrafts, satellite, and space-probe as beta source for solar-system explorations such as Mars science laboratory (MSL)/Curiosity, Europa (Moon of Jupiter) mission, asteroid, and comet missions.

The cost and the thermal power of the used energy source, however, are important factors to consider when recommending a suitable energy source. In this work, the calculation and simulation results for cross-section, integral yield, activity and yield of product show that the most suitable target material for production of cobalt-60 is Ni. Thus, <sup>61</sup>Ni(d, <sup>3</sup>He), <sup>62</sup>Ni(p, <sup>3</sup>He), and <sup>62</sup>Ni(d, α) reactions are the most suitable reactions and the appropriate energy of these reactions for formation of cobalt-60 is within the ranges of 25 MeV to 70 MeV, 30 MeV to 80 MeV, and

40 MeV to 85 MeV, respectively. The radioisotopes produced via the triton-induced reactions such as  $^{61}\text{Ni}(t, \alpha)$  and  $^{60}\text{Ni}(t, ^3\text{He})$  are quite expensive. The calculated data are, generally, of considerable importance in the production of radionuclides via particle accelerator for space, energy, and the medical researches. Those data lead the way to the experimenters in interdisciplinary science and technology.

## REFERENCES

- [1] Qaim, S. M., *et al.*, Excitation Function of the  $^{192}\text{Os}(^3\text{He}, 4n)$ -Reaction for Production of  $^{191}\text{Pt}$ , *Appl. Radiat. Isot.*, 67 (2009), June, pp. 1074-1077
- [2] Artun, O., Investigation of the Production of Promethium-147 via Particle Accelerator, *Indian J. Phys.* 91 (2017), 8, pp. 909-914
- [3] Calabretta, L. G., *et al.*, A Novel Superconducting Cyclotron for Therapy and Radioisotope Production, *Nucl. Instrum. Meth. Phys. Res. A*, 562 (2006), June, pp. 1009-1012
- [4] Tarkanyia, F., *et al.*, Activation Cross-Sections of Longer-Lived Radioisotopes of Deuteron Induced Nuclear Reactions on Terbium up to 50 MeV, *Nucl. Instrum. Meth. Phys. Res. B*, 316 (2013), Dec., pp. 183-191
- [5] Aslam, M. N., Qaim, S. M., Nuclear Model Analysis of Excitation Functions of Proton and Deuteron Induced Reactions on  $^{64}\text{Zn}$  and  $^3\text{He}$ - and  $\alpha$ -Particle Induced Reactions on  $^{59}\text{Co}$  Leading to the Formation of Copper-61: Comparison of Major Production Routes, *Appl. Radiat. Isot.*, 94 (2014), Dec., pp. 131-140
- [6] Artun, O., Aytakin, H., Calculation of Excitation Functions of Proton, Alpha and Deuteron Induced Reactions for Production of Medical Radioisotopes 122-125I, *Nucl. Instrum. Meth. Phys. Res. B*, 345 (2015), Feb., pp. 1-8
- [7] Artun, O., Estimation of the Production of Medical Ac-225 on Thorium Material via Proton Accelerator, *Appl. Radiat. Isot.* 127 (2017), Sept., pp. 166-172
- [8] Artun, O., A Study of Nuclear Structure for  $^{244}\text{Cm}$ ,  $^{241}\text{Am}$ ,  $^{238}\text{Pu}$ ,  $^{210}\text{Po}$ ,  $^{147}\text{Pm}$ ,  $^{137}\text{Cs}$ ,  $^{90}\text{Sr}$ , and  $^{63}\text{Ni}$  Nuclei Used in Nuclear Battery, *Mod. Phys. Lett. A*, 32 (2017), 22, p. 1, 13 p
- [9] Qaim, S. M., Nuclear Data for Production and Medical Application of Radionuclides: Present Status and Future Need, *Nucl. Med. Biol.*, 44 (2017), Jan., pp. 31-49
- [10] Wooten, A. L., *et al.*, Cross-Sections for  $(p, x)$  Reactions on Natural Chromium for the Production of  $^{52,52m,54}\text{Mn}$  Radioisotopes, *Appl. Radiat. Isot.*, 96 (2015), Feb., pp. 154-161
- [11] Uddin, M. S., *et al.*, Excitation functions of  $\alpha$ -Particle Induced Reactions on Enriched  $^{123}\text{Sb}$  and  $^{nat}\text{Sb}$  for Production of  $^{124}\text{I}$ , *Appl. Radiat. Isot.*, 69 (2011), Apr., pp. 699-704
- [12] Medvedev, D. G., *et al.*, Tailoring Medium Energy Proton Beam to Induce Low Energy Nuclear Reactions in  $^{86}\text{SrCl}_2$  for Production of PET Radioisotope  $^{86}\text{Y}$ , *Appl. Radiat. Isot.*, 101 (2015), July, pp. 20-26
- [13] Wooten, H. O., *et al.*, Benchmark IMRT Evaluation of a Co-60 MRI-Guided Radiation Therapy System, *Radiother. Oncol.*, 114 (2015), Mar., pp. 402-405
- [14] Hung, T. V., Khac, T., Dose Mapping Using MCNP Code and Experiment for SVST-Co-60/B Irradiator in Vietnam, *Appl. Radiat. Isot.*, 68 (2010), June, pp. 1104-1107
- [15] Qaim, S. M., *et al.*, Yield and Purity of  $^{82}\text{Sr}$  Produced via the  $^{nat}\text{Rb}(p, xn)^{82}\text{Sr}$  Process, *Appl. Radiat. Isot.*, 65 (2007), Feb., pp. 247-252
- [16] Mucic, S., *et al.*, The View Ray System: Magnetic Resonance-Guided and Controlled, *Radiotherapy Radiat. Oncol.*, 24 (2014), July, pp. 196-199
- [17] Yong, J. S., *et al.*, Dosimetric Impact of Applicator Displacement during High Dose Rate (HDR) Cobalt-60 Brachytherapy for Cervical Cancer: A Planning Study, *Radiat. Phys. and Chem.*, 119 (2016), Feb., pp. 264-271
- [18] Tarkany, F., *et al.*, Investigation of Excitation Functions of Alpha Induced Reactions on  $^{nat}\text{Xe}$ : Production of the Therapeutic Radioisotope  $^{131}\text{Cs}$ , *Nucl. Instrum. Meth. Phys. Res. B*, 267 (2009), Mar., pp. 742-254
- [19] Qaim, S. M., Radiochemical Determination of Nuclear Data for Theory and Applications, *J. Radioanal. Nucl. Chem.*, 284 (2010), Feb., pp. 489-505
- [20] Lange, R. G., Carroll, W. P., Review of Recent Advances of Radioisotope Power Systems, *Energy Convers. Manage.*, 49 (2008), Mar., pp. 393-401
- [21] Bennett, G. L., Mission Interplanetary: Using Radioisotope Power to Explore the Solar System, *Energy Convers. Manage.*, 49 (2008), Mar., pp. 382-392
- [22] \*\*\*, National Research Council, Radioisotope Power Systems, The National Academies Press, Washington DC, USA 2009
- [23] Prelas, M. A., *et al.*, A Review of Nuclear Batteries, *Prog. Nucl. Energy*, 75 (2014), Aug., pp. 117-148
- [24] Doherty, B. J., M. Sc. thesis, Massachusetts Institute of Technology, Cambridge, Mass. USA, 1969
- [25] Koning, A., *et al.*, Talys 1.8, <http://www.talys.eu/2015>
- [26] Artun, O., X-Particle the Mass Stopping Power Program 1.0 (X-PMSP), <http://www.x-pmsp.com>, 2017
- [27] \*\*\*, Exfor, Experimental Nuclear Reaction Data, <https://www-nds.iaea.org/exfor/exfor.htm>, 2017
- [28] \*\*\*, Tendl, Talys-Based Evaluated Nuclear Data Library, [https://tendl.web.psi.ch/tendl\\_2015/tendl\\_2015.html](https://tendl.web.psi.ch/tendl_2015/tendl_2015.html), 2015
- [29] Detroi, F., *et al.*, Investigation Deuteron-Induced Reactions on Cobalt, *Nucl. Instrum. Meth. Phys. Res. B*, 268 (2010), Jul., pp. 2571-2577
- [30] Levkovski, V. N., Cross-Sections of Medium Mass Nuclide Activation ( $A = 40-100$ ) by Medium Energy Protons and Alpha-Particles ( $E = 10-50$  MeV), Act. Cs. by Protons and Alphas, Moscow, 1991

Received on May 6, 2017

Accepted on November 3, 2017

**Озан АРТУН**

**ИСПИТИВАЊЕ ПРОИЗВОДЊЕ КОБАЛТА-60 АКЦЕЛЕРАТОРОМ ЧЕСТИЦА**

У овом раду симулиран је процес производње кобалта-60 акцелератором честица у опсегу енергија од 5 до 100 MeV, при јачини струје снопа честица од 1 mA и времену озрачивања од једног сата, како би се прорачунао принос по реакцији, активност реакције и интегрални принос за реакције индуковане наелектрисаним честицама. У складу са процесима нуклеарних реакција, резултати добијени у процесу производње кобалта-60 детаљно су размотрени да би се одредио одговарајући материјал за мету, оптимални опсег енергија и одговарајуће реакције.

*Кључне речи: акцелератор честица, нуклеарна реакција, активност, принос*

---